Hybrid stars in a relativistic quark model

Gautam Mitra,[1] Himanshu S. Sahoo,[1] Rabindranath Mishra,[1] and Prafulla K. Panda[2]
[1]*Department of Physics, Ravenshaw University, Cuttack 753 003, India*
[2]*Department of Physics, Utkal University, Bhubaneswar 751 004, India*

(Received 2 November 2021; accepted 25 February 2022; published 4 April 2022)

The phase transition of hadronic matter to deconfined quark matter in the interior of the neutron star is studied. A relativistic quark model is used to describe the hadronic matter whereas the MIT bag model is used to represent the quark matter. The coexistence of hadron-quark mixed phase in equilibrium is also investigated. The equation of state with nucleon + quark (NP-hybrid) and nucleon + hyperon + quark (NP + hyp-hybrid) matter is developed and stellar properties, such as the maximum mass, radii, tidal deformability, and gravitational redshift are determined. The behavior of the speed of sound and the adiabatic index in the hybrid matter are also studied. It is found that within the conformal limits of the speed of sound, stars below the 2-$M_\odot$ limit lack a sizable quark core but exhibit mixed phase of hadrons and quarks.

DOI: 10.1103/PhysRevC.105.045802

I. INTRODUCTION

Neutron stars are dense astronomical objects formed after the gravitational collapse of massive stars and often serve as astrophysical laboratories to study the behavior of nuclear matter at low temperature and high densities [1]. The structural investigation of a neutron star reveals two parts: the crust and the core [1]. At the crust of the neutron star where the density is comparable to the saturation density of nuclear matter ($\rho_0 = 0.15$ fmi^{-3}), its content is almost hadronic. As we proceed further inside the star, i.e., towards its core, the density increases and, hence, there arises the possibility of appearance of exotic matter [2–7]. At very high densities, there is the probability of overlapping of baryons leading to phase transition with deconfined quark matter. Moreover, three flavored quarks are energetically more favored than hadronic matter [8,9].

This possibility is further strengthened from the fact that formation of exotic matter, such as hyperons leads to softening of equation of state (EoS) and a reduction in maximum mass of the neutron star [10–12], very often referred to as a "hyperon puzzle" (see Ref. [13] and the references therein for a wonderful review on EoS of neutron stars). One of the driving mechanisms of the hyperon puzzle is the phase transition from hadronic to deconfined quark matter [14–16]. At sufficiently high-energy density, quantum chromodynamics calculations also predict the same results, i.e., when the density of nuclear matter exceeds nuclear saturation density there may appear hyperonic degrees of freedom, and if the density increases further, deconfinement of hadronic matter into quark matter may occur ultimately resulting in quark-gluon plasma as observed in ultrarelativistic heavy-ion collision experiments carried out at the Relativistic Heavy Ion Collider and the Large Hadron Collider [17–22]. Even after decades of studying phase transition inside neutron stars, it is still not clear whether quark matter exists in the core of the neutron star and if at all quarks exist inside neutron stars, then at what point the hadron-quark phase transition occurs. Recently, after analyzing about 570 000 EoSs using a unique "speed-of-sound" interpolation, Annala *et al.* [23] predicted the existence of a substantial quark core in highly massive neutron stars ($>2M_\odot$).

In the present paper we explore the possibility of occurrence of hadron-quark phase transition in neutron stars using EoS's developed from the quark level. The description of the composition and properties of the neutron stars depends upon the appropriate usage of EoS describing its crust and core region [24]. However, there does not exist a unified theory which could explain both the hadronic and quark phases in all ranges of densities and pressure. Therefore, in order to study the different phases of matter at such extremities it is suitable to calculate the EoS of hadronic phase and quark phase separately from their independent theories and then construct the phase transition between them. In this paper, the hadron-quark phase transition is studied by incorporating proper theories for the hadronic phase and quark phase separately.

The hadronic matter can be described using different approaches [13], such as the *ab initio* methods which include the (Dirac) Brueckner-Hartree-Fock approach, approaches based on the variational method, self-consistent Green's function method, chiral effective field theory approach [25], and quantum Monte Carlo methods. Other approaches include the relativistic mean-field models, such as the Walecka model [26] and phenomenological models with effective density-dependent interactions, such as the Skyrme models [27]. All these approaches treat baryons as structureless point objects. Various studies have been developed with the inclusion of quark structure of baryons with the meson interactions described at the quark level. The quark-meson coupling (QMC) model [28–30] has been widely used to study the nuclear and neutron star matter. The QMC model along with the MIT bag model have also been used [31–35] to study phase transition in neutron stars.

In this paper, the hadronic matter present inside the star is described using a relativistic quark model [36–41], alternatively called the modified quark-meson coupling model (MQMC). The MQMC model takes into consideration the quark substructure of the hadrons. It is a potential model in which the quarks inside the baryons are considered to be independently confined by a phenomenological average potential with an equally mixed scalar-vector harmonic form. The interaction between the baryons are realized through coupling of quarks to σ, ω, and ρ mesons in mean-field approximations. The quark matter inside neutron stars is described using the quark-meson coupling model (also called the bag model) [28–30] in which the quarks are assumed to be confined inside the bag by neutralization of the inner quark pressure and the outer bag pressure. The choice of such models for describing the phase transition of hadronic matter to quark matter is evident from the fact that both models use quark degrees of freedom to develop the EoS. Furthermore, both the MQMC model [36–43] and the bag model [28–30,44–48] have been widely successful in describing various properties of symmetric and asymmetric nuclear matter as well as neutron stars.

Using the above formalisms we analyze the phase transition from hadronic to quark matter by applying the Gibbs criteria ensuring conservation of global baryon number and global electric charge. Gibbs equilibrium condition of hadronic and quark phases also dictates that they must have equal baryon chemical potentials and pressures but different electron chemical potentials [49]. The presence of mixed phase of both hadronic matter and quark matter in the interior of the neutron star is also studied. The effect of hadron-quark phase transition on the observational properties of neutron stars are analyzed and compared with the current multimessenger observations obtained post GW170817 gravitational wave event [50–53] and the neutron star interior composition explorer mission (NICER) observations [54,55] of PSR J0740 + 6620. In the light of the prediction of Annala *et al.* [23] of a sizeable quark core in massive neutron stars, we study the variation in speed of sound and adiabatic index in hybrid star matter.

The paper is organized as follows: In Sec. II we provide a brief description of the MQMC model and develop the EoS of hadronic matter. Sections III and IV describe the formalism for quark matter and mixed matter whereas the results are discussed in Sec. V.

II. MODEL

A. Hadronic matter

The hadronic sector is realized using the modified quark-meson coupling model in which the quarks inside the baryons are confined by a phenomenological flavor-independent potential $U(r)$ and the baryon-baryon interaction occurs via the exchange of effective σ, ω, and ρ fields [36,38]. The potential $U(r)$ has the form

$$U(r) = \tfrac{1}{2}(1+\gamma^0)V(r),$$

with

$$V(r) = (ar^2 + V_0), \quad a > 0, \tag{1}$$

where $(a,\ V_0)$ are the potential parameters. The Dirac equation involving the quark field $\psi_q(\mathbf{r})$ in terms of coupling constants g^q_σ, g^q_ω, and g^q_ρ and the meson fields σ_0, ω_0, and b_{03} is given by

$$\left[\gamma^0\left(\epsilon_q - V_\omega - \tfrac{1}{2}\tau_{3q}V_\rho\right) - \vec{\gamma}\cdot\vec{p} - (m_q - V_\sigma) - U(r)\right] \times \psi_q(\vec{r}) = 0, \tag{2}$$

where $V_\sigma = g^q_\sigma\sigma_0$, $V_\omega = g^q_\omega\omega_0$, and $V_\rho = g^q_\rho b_{03}$. m_q is the quark mass and τ_{3q} is the third component of the Pauli matrices. The effective quark energy and the effective quark mass can be written as

$$\epsilon^*_q = \epsilon_q - V_\omega - \tfrac{1}{2}\tau_{3q}V_\rho \quad \text{and} \quad m^*_q = m_q - V_\sigma. \tag{3}$$

The ground-state quark energy is obtained from the eigenvalue condition,

$$(\epsilon'_q - m'_q)\sqrt{\frac{\lambda_q}{a}} = 3, \tag{4}$$

where

$$\epsilon'_q = (\epsilon^*_q - V_0/2) \quad \text{and} \quad m'_q = (m^*_q + V_0/2), \tag{5}$$

and

$$\lambda_q = (\epsilon'_q + m'_q). \tag{6}$$

The solution of Eq. (4) for the quark energy ϵ^*_q immediately leads to the mass of baryon in the medium in zeroth order as

$$E^{*0}_B = \sum_q \epsilon^*_q. \tag{7}$$

Incorporating the spurious center-of-mass (c.m.) correction $\epsilon_{\text{c.m.}}$, the pionic correction δM^π_B for restoration of chiral symmetry, and the short-distance one-gluon exchange contribution $(\Delta E_B)_g$ to the zeroth-order baryon mass in the medium, the effective mass of the baryon in the medium becomes [36,38,39]

$$M^*_B = E^{*0}_B - \epsilon_{\text{c.m.}} + \delta M^\pi_B + (\Delta E_B)^E_g + (\Delta E_B)^M_g. \tag{8}$$

B. The equation of state

The total energy density and pressure at a particular baryon density for the nuclear matter in β equilibrium can be found as

$$\mathcal{E} = \frac{1}{2}m^2_\sigma\sigma^2_0 + \frac{1}{2}m^2_\omega\omega^2_0 + \frac{1}{2}m^2_\rho b^2_{03} \tag{9a}$$

$$+ \frac{\gamma}{2\pi^2}\sum_B \int^{k_{f,B}} \left[k^2 + M^{*2}_B\right]^{1/2} k^2 dk$$

$$+ \sum_l \frac{1}{\pi^2}\int_0^{k_l} \left[k^2 + m^2_l\right]^{1/2} k^2 dk, \tag{9b}$$

$$P = -\frac{1}{2}m^2_\sigma\sigma^2_0 + \frac{1}{2}m^2_\omega\omega^2_0 + \frac{1}{2}m^2_\rho b^2_{03}$$

$$+ \frac{\gamma}{6\pi^2}\sum_B \int^{k_{f,B}} \frac{k^4\, dk}{\left[k^2 + M^{*2}_B\right]^{1/2}}$$

$$+ \frac{1}{3}\sum_l \frac{1}{\pi^2}\int_0^{k_l} \frac{k^4 dk}{\left[k^2 + m^2_l\right]^{1/2}}, \tag{9c}$$

where $\gamma = 2$ is the spin degeneracy factor for nuclear matter, $B = N, \Lambda, \Sigma^{\pm}, \Sigma^{0}, \Xi^{-}, \Xi^{0}$, $l = e, \mu$ whereas the total baryon density $\rho_B = \rho_p + \rho_n$. The vector mean-fields ω_0 and b_{03} are determined through

$$\omega_0 = \frac{g_\omega}{{m_\omega}^2} \sum_B x_{\omega B} \rho_B, \quad b_{03} = \frac{g_\rho}{2{m_\rho}^2} \sum_B x_{\rho B} \tau_{3B} \rho_B, \tag{10}$$

where $g_\omega = 3g_\omega^q$ and $g_\rho = g_\rho^q$.

The scalar mean-field σ_0 is fixed by

$$\frac{\partial \mathcal{E}}{\partial \sigma_0} = 0. \tag{11}$$

The isoscalar scalar and isoscalar vector couplings g_σ^q and g_ω are fitted to the saturation density and binding energy for nuclear matter. The isovector vector coupling g_ρ is set by fixing the symmetry energy. For a given baryon density, ω_0, b_{03}, and σ_0 are calculated from Eqs. (10) and (11), respectively. For the matter to be charge neutral, the total charge after deleptonization must vanish, i.e.,

$$q_{\rm tot} = \sum_B q_B \frac{\gamma k_B^3}{6\pi^2} + \sum_{l=e,\mu} q_l \frac{k_l^3}{3\pi^2} = 0, \tag{12}$$

where q_B corresponds to the electric charge of baryon species B and q_l corresponds to the electric charge of lepton species l.

Since the strangeness quantum number is not conserved in a star, the net strangeness is determined by the condition of β equilibrium which for baryon B is then given by $\mu_B = b_B \mu_n - q_B \mu_e$, where b_B is its baryon number and μ_B is the chemical potential of baryon B, defined as

$$\mu_B = \sqrt{k_B^2 + M_B^{*2}} + g_\omega \omega_0 + g_\rho \tau_{3B} b_{03}, \tag{13}$$

where τ_{3B} is the isospin projection of baryon B. Thus, the chemical potential of any baryon can be obtained from the two independent chemical potentials μ_n and μ_e of neutron and electron, respectively.

The lepton Fermi momenta are the positive real solutions of $(k_e^2 + m_e^2)^{1/2} = \mu_e$ and $(k_\mu^2 + m_\mu^2)^{1/2} = \mu_\mu$. The equilibrium composition of the star is obtained by solving the equations of motion of meson fields in conjunction with the charge neutrality condition, given in Eq. (12) at a given total baryonic density $\rho = \sum_B \gamma k_B^3/(6\pi^2)$.

III. QUARK MATTER

The quark matter is described using the bag model where quarks are confined inside the bag by neutralization of the pressure exerted by the quarks inside the bag and the bag pressure exerted on the bag walls from outside the bag. The matter is assumed to be in a state of chemical equilibrium with

$$\mu_d = \mu_s = \mu_u + \mu_e, \tag{14}$$

where

$$\mu_u = \tfrac{1}{3}\mu_n - \tfrac{2}{3}\mu_e, \tag{15}$$

$$\mu_d = \tfrac{1}{3}\mu_n + \tfrac{1}{3}\mu_e, \tag{16}$$

$$\mu_s = \tfrac{1}{3}\mu_n + \tfrac{1}{3}\mu_e, \tag{17}$$

μ_n and μ_e being two independent chemical potentials. The pressure corresponding to u, d, and s quarks are given by

$$P_q = \frac{1}{4\pi^2} \sum_i \left[\mu_i k_i \left({\mu_i}^2 - \frac{5}{2} m_i^2 \right) + \frac{3}{2} m_i^4 ln \frac{\mu_i + k_i}{m_i} \right], \tag{18}$$

where

$$k_i = \left(\mu_i^2 - m_i^2 \right)^{1/2}, \tag{19}$$

with $i = u, d$, and s.

The lepton pressure is

$$P_l = \frac{1}{3\pi^2} \sum_l \int_0^{k_l} \frac{k^4 dk}{\left(k^2 + m_l^2 \right)^{1/2}}. \tag{20}$$

Total pressure is, thus, the sum of quark pressure and lepton pressure minus the bag pressure,

$$P = P_q + P_l - B. \tag{21}$$

Similarly, the energy density for quark matter is given by [56],

$$\mathcal{E}_q = B + \frac{3}{4\pi^2} \sum_i \left[\mu_i k_i \left(\mu_i^2 - \frac{1}{2} m_i^2 \right) - \frac{1}{2} m_i^4 ln \frac{(\mu_i + k_i)}{m_i} \right]. \tag{22}$$

IV. MIXED MATTER

In the intermediate layers of the neutron stars, matter is assumed to be composed of a charge neutral mixture of hadrons and quarks. The condition for charge neutrality of neutron star matter composed of hadrons, quarks, and leptons is as follows:

$$\chi \rho^{\rm QM} + (1 - \chi) \rho^{\rm HM} + \rho^l = 0. \tag{23}$$

Here, $\rho^{\rm QM}$ and $\rho^{\rm HM}$ represent the charge densities of quark matter and hadronic matter. χ and $(1 - \chi)$ represent the fractional volume of mixed matter occupied by quark and hadronic phases, respectively.

The phase boundary where both the hadronic and the quark matter coexists is determined by using the Gibbs criteria. The critical pressure and chemical potential are given by the condition,

$$\mu_{\rm HM} = \mu_{\rm QM}, \tag{24}$$

and

$$P_{\rm HM}(\mu_B) = P_{\rm QM}(\mu_B). \tag{25}$$

The energy and the total baryon densities in the mixed phase are given by

$$\mathcal{E}_q = \chi \mathcal{E}^{\rm QM} + (1 - \chi) \mathcal{E}^{\rm HM} + \mathcal{E}^l, \tag{26}$$

$$\rho = \chi \rho^{\rm QM} + (1 - \chi) \rho^{\rm HM}. \tag{27}$$

Once the EoS are determined for the three phases of matter, it becomes easier to compute the mass and radius of the neutron star by integrating the Tolman-Oppenheimer-Volkoff (TOV) equations [57] from the origin as an initial

TABLE I. MQMC potential parameter V_0 for different baryons with quark mass $m_u = m_d = 200$ and $m_s = 280$ MeV, with $a = 0.722\,970$ fm^{-3}.

Baryon	M_B (MeV)	V_0 (MeV)
N	939	5.44
Λ	1115.6	35.18
Σ	1193.1	50.78
Ξ	1321.3	67.13

value problem for a given choice of the central energy density (ε_0),

$$\frac{dP}{dr} = -\frac{G(Mc^2 + 4\pi r^3 P)(\mathcal{E} + P)}{rc^4(r - 2GM/c^2)}, \tag{28}$$

$$\frac{dM}{dr} = 4\pi r^2 \frac{\mathcal{E}}{c^2}, \tag{29}$$

where G is the gravitational constant and $M(r)$ is the enclosed gravitational mass. Of particular importance is the maximum mass obtained from the solution of the TOV equations. The value of $r\,(=R)$ where the pressure vanishes defines the surface of the star. We may note here that to properly describe the crust of the star where the density is significantly smaller than the nuclear saturation density, we add the standard Baym-Pethick-Sutherland [58] EoS to the EoS developed above.

V. RESULTS AND DISCUSSIONS

We start with two possible compositions of neutron star matter in the hadronic sector using the MQMC model, i.e., matter containing nucleons only (NP) and matter containing both nucleons and hyperons (NP + hyp). The MQMC model parameters are fixed to determine the EoS of the hadronic composition. The two potential parameters a and V_0 in the MQMC model are obtained by fitting the nucleon mass $M_N = 939$ MeV and charge radius of the proton $\langle r_N \rangle = 0.84$ fm in free space. The potential parameter V_0 obtained for different baryons with quark mass $m_u = m_d = 200$ and $m_s = 280$ MeV, with $a = 0.722\,970$ fmi^{-3} are tabulated in Table I.

The quark meson couplings g_σ^q, $g_\omega = 3g_\omega^q$, and $g_\rho = g_\rho^q$, given in Table II, are fitted self-consistently for the nucleons to obtain the correct saturation properties of nuclear matter binding energy $E_{\text{B.E.}} \equiv B_0 = \mathcal{E}/\rho_B - M_N = -15.7$ MeV, pressure $P = 0$, and symmetry energy $J = 32.0$ MeV at $\rho_B = \rho_0 = 0.15$ fm^{-3}. The hyperon-ω coupling are fixed by determining $x_{\omega B}$ obtained from hyperon potentials in nuclear matter, $U_B = -(M_B - M_B^*) + x_{\omega B} g_\omega \omega_0$ where $B = \Lambda$, Σ, and Ξ with $U_\Lambda = -28$, $U_\Sigma = 30$, and $U_\Xi = -10$ MeV. For fixed

TABLE II. The quark-meson couplings g_σ^q, g_ω, and g_ρ for quark mass $m_q = 200$ MeV.

m_q (MeV)	g_σ	g_ω	g_ρ
200	4.368	7.405	8.733

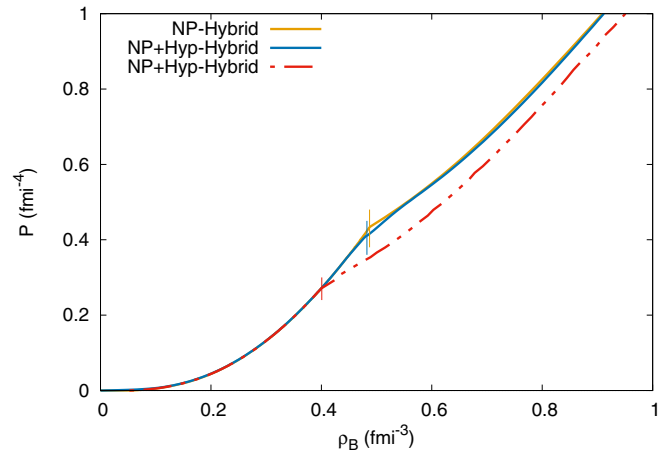

FIG. 1. Pressure as a function of density for NP-hybrid and NP + hyp-hybrid matter. The dashed curve represents the EoS for $B^{1/4} = 200$ MeV. The vertical dashes indicate the transition points from hadronic to mixed phase for the respective cases.

$x_{\rho B} = 1$, we obtain [39] $x_{\omega\Lambda} = 0.825\,41$, $x_{\omega\Sigma} = 1.453\,53$, and $x_{\omega\Xi} = 0.525\,41$.

For the quark sector we use the bag model with the bag constant fixed at $B^{1/4} = 210$ MeV, whereas the quark mass is fixed at $m_u = m_d = 5$ and $m_s = 150$ MeV. To study the effect of the bag constant, $B^{1/4}$ is varied [59] to 200 MeV and compared with the results of 210 MeV. Having fixed all the required parameters in both models, we determine the EoS of both hadronic and quark sectors to obtain two possible compositions, NP-hybrid indicating matter containing nucleons and quarks, and NP + hyp-hybrid with nucleons, hyperons, and quarks.

Figure 1 shows the EoS of matter inside the neutron star. We observe the existence of a mixed phase of hadronic and quark matter for both nucleonic (NP-hybrid) and hyperonic compositions (NP + hyp-hybrid). With $B^{1/4} = 210$ MeV for both compositions, the mixed phase appears at a density (0.48 fm^{-3}) whereas for $B^{1/4} = 200$ MeV, the transition density is (0.40 fm^{-3}). Furthermore, a decrease in the bag constant softens the EoS.

In Fig. 2, we plot the particle fraction as a function of baryon density for NP + hyp-hybrid composition with $B^{1/4} = 210$ MeV. In accordance with the β equilibrium condition, at nuclear matter density below saturation density, β decay of neutrons to muons decreases the neutron concentration and simultaneously increases the muon population. The concentration of electron and muon increases up to a density of $2.9\rho_0$, thereafter, their population decreases with an increase in density. Although hyperons start to appear at around this density ($2.9\rho_0$), the quarks begin to form at $3.2\rho_0$, indicating the transition from hadronic phase to mixed phase. Appearance of negative baryon species at the expense of lepton population is obvious for the maintenance of charge neutrality condition of nuclear matter. Thus, the matter beyond $3.2\rho_0$ can be thought of to exist as a mixed phase of both hadron and quark matter in equilibrium. It is also noted from Fig. 2 that the Σ hyperon is absent in the matter distribution for the given

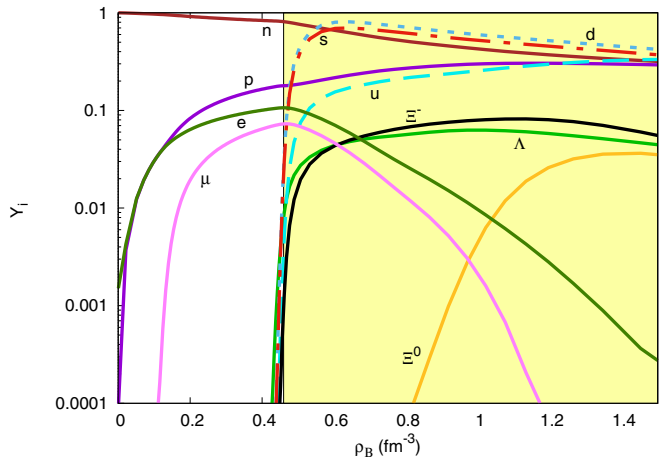

FIG. 2. Particle fraction as a function of total baryon density for $B^{1/4} = 210$ MeV. The shaded part shows the mixed phase region.

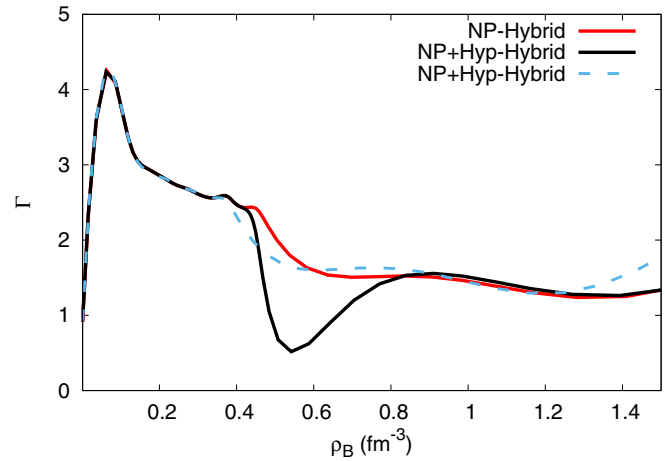

FIG. 4. Adiabatic index as a function of density. The continuous lines are for $B^{1/4} = 210$ MeV and the dashed line represents $B^{1/4} = 200$ MeV.

set of hyperon potentials since we have chosen a repulsive potential of $U_\Sigma = 30$ MeV for it.

The speed of sound $c_s^2 = \frac{dP}{d\mathcal{E}}$ plays an important role in characterizing the dense neutron star matter. Models based on nonrelativistic theories predict $c_s \ll 1$, whereas ultrarelativistic theory based models involving massless particles predict $(c_s)^2 = 1/3$. Attribution of mass to the particles lowers the value of speed of sound to $(c_s)^2 < 1/3$. So, it is obvious to apprehend the value of speed of sound for intermediate densities $(c_s)^2 \leqslant 1/3$ [60]. Since neutron star matter falls within this intermediate range of densities, i.e., 1–10 times nuclear matter saturation density, therefore, it is interesting to determine the speed of sound.

Figure 3 shows the variation of speed of sound squared with baryon density for $B^{1/4} = 210$ and $B^{1/4} = 200$ MeV. As the matter density increases within the neutron star, the velocity of sound increases monotonously and up to around three times ρ_0, approaches the conformal limit $(c_s)^2 \leqslant 1/3$ for

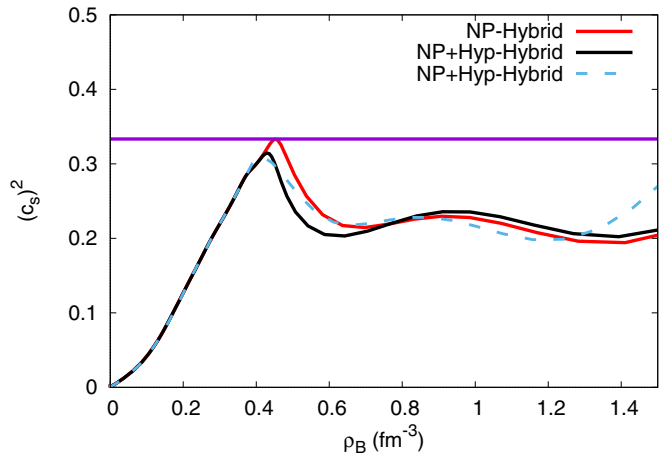

FIG. 3. The square of the speed of sound as a function of density in the two possible dense matter compositions. The continuous lines are for $B^{1/4} = 210$ MeV and the dashed line represents $B^{1/4} = 200$ MeV. The horizontal line indicates the conformal limit.

both NP-hybrid and NP + hyp-hybrid matter. Corresponding to the transition point from hadron phase to mixed phase at around 0.48 fm^{-3} there occurs a sudden decrease in the speed of sound. Throughout the density range the speed of sound remains within the conformal limit. Such compliance of the speed of sound with the conformal limit suggests [23] the presence of a sizable quark core in massive stars ($M \approx 2\ M_\odot$). In the present paper, the maximum mass is below 2 $M_\odot$ with no pure quark core.

The adiabatic index $\Gamma = (\rho_B/P)(dP/d\rho_B)$ determines the change in pressure associated with change in local baryon density and plays a crucial role in determining the stability of a star as well as indicates possible phase changes in neutron star matter. Figure 4 shows the variation of adiabatic index with baryon density. The jumps are associated with densities involving changes in the composition of the matter.

In Fig. 5, we plot the gravitational mass of the star as a function of the radius with the observational limits on the maximum mass from the pulsars PSR J1614-2230 and PSR J0740 + 6620 shown in the shaded regions. The most massive star is obtained for purely nucleonic composition with a mass of 2.1 $M_\odot$, which falls significantly to 1.86 $M_\odot$ with phase transition to mixed matter. The corresponding radius comes out to 12.81 km. With the inclusion of hyperons, the maximum mass becomes 1.85 $M_\odot$, and the corresponding radius is 12.80 km. For $B^{1/4} = 200$ MeV, the maximum mass further reduces to 1.73 $M_\odot$ with the corresponding radius of 12.65 km.

The results are given in Table III. Although the mass of PSR J1614-2230 has been determined to $1.928 \pm 0.017\ M_\odot$ [61], the mass of the pulsar PSR J0740 + 6620 from NICER observations has recently been updated [54,55,62] to $2.08 \pm 0.07\ M_\odot$ with the corresponding radius being $13.7^{+2.6}_{-1.5}$ km in one study [54] and $12.39^{+1.30}_{-0.98}$ km in another [55]. The canonical radius $R_{1.4}$ of 13.6 km for NP-hybrid and NP + hyp-hybrid lies within recent NICER measurements of the pulsar PSR J0030 + 0451.

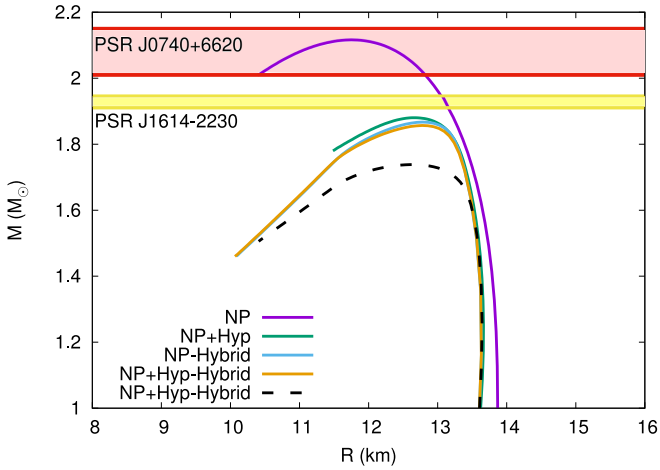

FIG. 5. Neutron star masses as a function of radius. The observational limits on the maximum mass from PSR J0740 + 6620 and PSR J1614-2230 are shown in the shaded regions. The dashed curve is for $B^{1/4} = 200$ MeV.

For a static spherically symmetric star of mass M and radius R, the tidal deformation parameter λ can be expressed in terms of the dimensionless Love number k_2 as

$$\lambda = \tfrac{2}{3}k_2R^5. \tag{30}$$

The tidal Love number k_2 is given by [63–65]

$$\begin{aligned} k_2 = {} & \tfrac{8}{5}\beta^5(1-2\beta)^2[2-y_R+2\beta(y_R-1)] \\ & \times\{2\beta[6-3y_R+3\beta(5y_R-8)] \\ & +4\beta^3[13-11y_R+\beta(3y_R-2) \\ & +2\beta^2(1+y_R)]+3(1-2\beta)^2 \\ & \times[2-y_R+2\beta(y_R-1)]\ln(1-2\beta)\}^{-1}, \end{aligned} \tag{31}$$

where $\beta \equiv GM/Rc^2$ is the dimensionless compactness parameter. The quantity $y_R \equiv y(R)$ satisfies the first-order differential equation,

$$\frac{dy}{dr} = -\frac{y^2}{r} - \frac{y-6}{r-2GM/c^2} - rQ, \tag{32}$$

with

$$\begin{aligned} Q = {} & \frac{4\pi G}{c^4}\frac{(5-y)\mathcal{E}+(9+y)P+(\mathcal{E}+P)/c_s^2}{1-2GM/c^2} \\ & -\left[\frac{2G(M+4\pi Pr^3/c^2)}{r(rc^2-2GM)}\right]^2. \end{aligned} \tag{33}$$

TABLE III. Maximum gravitational mass M ($M_\odot$), radius R (km), and $R_{1.4}$ (km) for different $B^{1/4}$s.

$B^{1/4}$ (MeV)	Composition	M ($M_\odot$)	R (km)	$R_{1.4}$ (km)	$\Lambda_{1.4}$
210	NP-hybrid	1.86	12.81	13.6	666
	NP + hyp-hybrid	1.85	12.80	13.6	663
200	NP + hyp-hybrid	1.73	12.65	13.6	662

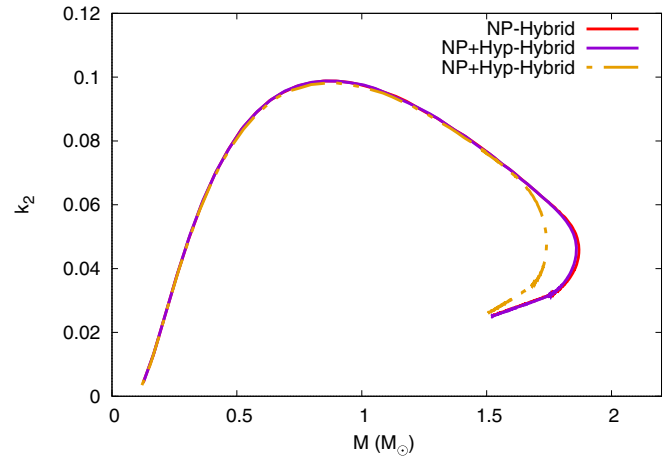

FIG. 6. Love number as a function of mass of the star for the two compositions. The dashed curve is for $B^{1/4} = 200$ MeV.

Equation (32) needs to be integrated self-consistently along with the TOV equations (29) with the boundary conditions at $r = 0$ such that $y(0) = 2$, $M(0) = 0$, and $P(0) = P_c$.

Figure 6 shows the variation of Love number k_2. It is observed that the value k_2 peaks near 1 $M_\odot$. For masses above and below the 1 $M_\odot$ range the k_2 value is lower due to less contribution of the tidal deformation on the quadrupole moment.

The dimensionless tidal deformability of a neutron star can be written in terms of the tidal Love number k_2 and the compactness parameter as

$$\Lambda_D = \frac{2}{3}k_2\left(\frac{R}{M}\right)^5. \tag{34}$$

In Fig. 7, the dimensionless tidal deformability Λ_D as a function of gravitational mass M of the star. We note a rapid fall of Λ_D as M increases. The fall in Λ_D is a combined effect of the change in Love number k_2 and the compactness parameter M/R caused by the appearance of the hadron-quark phase transition. For a hybrid star with NP and NP + hyp, the values

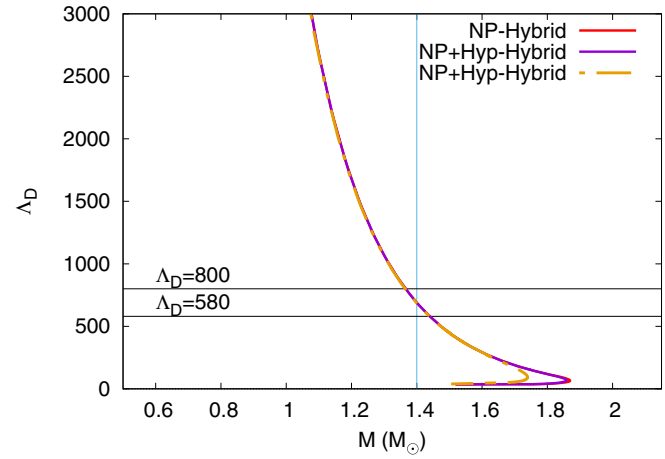

FIG. 7. The dimensionless tidal deformability as a function of star mass. The dashed curve is for $B^{1/4} = 200$ MeV.

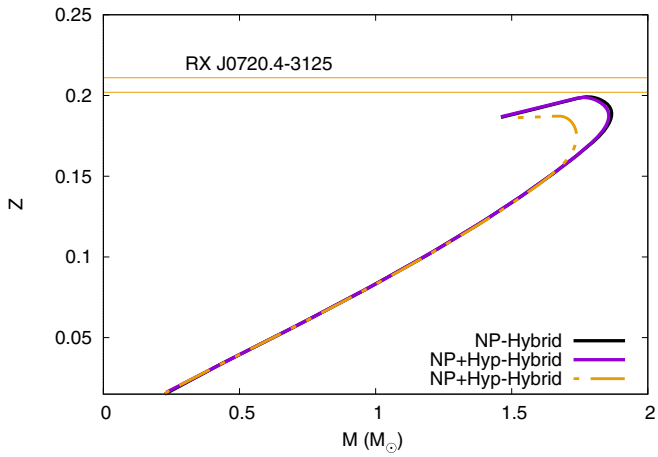

FIG. 8. Gravitational redshift as function of star mass. Also shown is the observational limit on redshift from the pulsar RX J0720.4-3125. The dashed line represents the curve for $B^{1/4} = 200$ MeV.

of Λ_D corresponding to canonical mass 1.4 $M_\odot$ are given in Table III.

The variation of gravitational redshift with gravitational mass is shown in Fig. 8. The gravitational redshift of a star is defined by

$$Z = \frac{1}{\sqrt{1 - 2GM/Rc^2}}. \tag{35}$$

Recent [66] observational limits imposed on redshift from RX J0720.4-3125, an isolated neutron star with a canonical radius of 13.3 ± 0.5 km and compactness of 0.105 ± 0.002, provide the range of ($Z = 0.205^{+0.006}_{-0.003}$) and is indicated by the yellow lines in Fig. 8. In the present paper, for $B^{1/4} = 210$ MeV, we obtain the value of $Z = 0.188$ for NP-hybrid matter and $Z = 0.187$ for the NP + hyp-hybrid case. For $B^{1/4} = 200$ MeV, Z decreases to $Z = 0.174$ due to the decrease in the mass of the star.

VI. CONCLUSION

In the present paper we have studied the possibility of hadron-quark phase transition in neutron stars using the MQMC model to describe the hadronic part and the bag model to describe the quark phase. The EoS is determined for two possible combinations of stellar matter, NP-hybrid indicating nucleonic and quark composition, and NP + hyp-hybrid having hyperons in addition to nucleons and quarks. Using the Gibbs construction with global charge neutrality conditions, a mixed phase of hadronic and quark matter is obtained at densities relevant to neutron stars, whereas a pure quark phase remains absent. We show the variation of the speed of sound and the adiabatic index for the hybrid EoS and find that the speed of sound lies below the conformal limit.

The various stellar properties, such as mass, radius, tidal deformability, and gravitational redshift are determined for two different bag constants. Within the above formalism, we obtain stars with maximum mass below 2 $M_\odot$. Studies on quark-hadron phase transitions in compact stars [67,68] which satisfy the 2 $M_\odot$ constraint suggest the need for strongly interacting quarks with contribution from color superconductivity or the presence of considerable repulsive vector interactions [69] in the quark matter for a stiffer quark matter EoS. Our studies agree with the conclusions of Ref. [23], suggesting a hadron-quark phase transition in matter showing conformal behavior as well as indicating the absence of a sizable quark core with stars below the 2 $M_\odot$ limit.

ACKNOWLEDGMENTS

We would like to acknowledge the computational facilities in the Department of Physics, Ravenshaw University, Cuttack set up from the financial assistance of BRNS, India vide Project No. 2013/37P/66/BRNS. H.S.S. would like to acknowledge support via CSIR-SRF Fellowship No. 09/1036/0007 (2018). P.K.P would like to acknowledge the financial assistance from DST(FIST), India for Project No. SR/FST/PS-II/2017/22.

[1] N. K. Glendenning, *Compact Stars, Nuclear Physics, Particle Physics and General Relativity* (Springer-Verlag, New York, 1997).
[2] A. Akmal, V. R. Pandharipande, and D. G. Ravenhall, Phys. Rev. C **58**, 1804 (1998).
[3] F. Weber, Prog. Part. Nucl. Phys. **54**, 193 (2005).
[4] W. Weise, Prog. Part. Nucl. Phys. **67**, 299 (2012).
[5] D. Chatterjee and I. Vidaña, Eur. Phys. J. A **52**, 29 (2016).
[6] H.-Y. Chen, P. M. Chesler, and A. Loeb, Astrophys. J. Lett. **893**, L4 (2020).
[7] A. Drago and G. Pagliara, Phys. Rev. D **102**, 063003 (2020).
[8] A. R. Bodmer, Phys. Rev. D **4**, 1601 (1971).
[9] E. Witten, Phys. Rev. D **30**, 272 (1984).
[10] N. Glendenning, Astrophys. J. **293**, 470 (1985).
[11] R. Knorren, M. Prakash, and P. J. Ellis, Phys. Rev. C **52**, 3470 (1995).
[12] M. Prakash, I. Bombaci, M. Prakash, P. J. Ellis, and J. M. Lattimer, Phys. Rep. **280**, 1 (1997).
[13] G. F. Burgio, H.-J. Schulze, I. Vidaña, and J.-B. Wei, Prog. Part. Nucl. Phys. **120**, 103879 (2021).
[14] T. Klähn, R. Łastowiecki, and D. Blaschke, Phys. Rev. D **88**, 085001 (2013).
[15] I. Bombaci *et al.*, Eur. Phys. J. A **52**, 58 (2016).
[16] K. Masuda, T. Hatsuda, and T. Takatsuka, Eur. Phys. J. A **52**, 65 (2016).
[17] F. Karsch, E. Laermann, and A. Peikert, Phys. Lett. B **478**, 447 (2000).
[18] F. Karsch (RBC and HotQCD Collaborations), J. Phys. G: Nucl. Part. Phys. **35**, 104096 (2008).
[19] S. Borsanyi, Z. Fodor, C. Hoelbling, S. D. Katz, S. Krieg, and K. K. Szabo, Phys. Lett. B **730**, 99 (2014).
[20] A. Bazavov, T. Bhattacharya, C. DeTar, H.-T. Ding, S. Gottlieb, R. Gupta, P. Hegde, U. M. Heller, F. Karsch, E. Laermann,

L. Levkova, S. Mukherjee, P. Petreczky, C. Schmidt, C. Schroeder, R. A. Soltz, W. Soeldner, R. Sugar, M. Wagner, and P. Vranas (HotQCD Collaboration), Phys. Rev. D **90**, 094503 (2014).
[21] M. Gyulassy and L. McLerran, Nucl. Phys. A **750**, 30 (2005).
[22] A. Andronic, P. Braun-Munzinger, K. Redlich, and J. Stachel, Nature (London) **561**, 321 (2018).
[23] E. Annala *et al.*, Nat. Phys. **16**, 907 (2020).
[24] P. Danielwicz, R. Lacey, and W. G. Lynch, Science **298**, 1592 (2002).
[25] R. J. Furnstahl, Lect. Notes Phys. **641**, 1 (2004).
[26] J. D. Walecka, Ann. Phys. (NY) **83**, 491 (1974).
[27] M. Dutra, O. Lourenço, J. S. Sá Martins, A. Delfino, J. R. Stone, and P. D. Stevenson, Phys. Rev. C **85**, 035201 (2012).
[28] P. A. M. Guichon, Phys. Lett. B **200**, 235 (1988).
[29] K. Saito and A. W. Thomas, Phys. Lett. B **327**, 9 (1994); **335**, 17 (1994); **363**, 157 (1995); Phys. Rev. C **52**, 2789 (1995).
[30] K. Saito, K. Tsushima, and A. W. Thomas, Nucl. Phys. A **609**, 339 (1996); Phys. Rev. C **55**, 2637 (1997); Phys. Lett. B **406**, 287 (1997).
[31] P. K. Panda, D. P. Menezes, and C. Providenĉia, Phys. Rev. C **69**, 025207 (2004).
[32] B. K. Sharma, P. K. Panda, and S. K. Patra, Phys. Rev. C **75**, 035808 (2007).
[33] G. F. Burgio, Nucl. Phys. A **749**, 337 (2005).
[34] H. Chen, M. Baldo, G. F. Burgio, and H.-J. Schulze, Phys. Rev. D **84**, 105023 (2011).
[35] H. Chen, J.-B. Wei, M. Baldo, G. F. Burgio, and H.-J. Schulze, Phys. Rev. D **91**, 105002 (2015).
[36] N. Barik, R. N. Mishra, D. K. Mohanty, P. K. Panda, and T. Frederico, Phys. Rev. C **88**, 015206 (2013).
[37] N. Barik and R. N. Mishra, Phys. Rev. D **61**, 014002 (1999).
[38] R. N. Mishra, H. S. Sahoo, P. K. Panda, N. Barik, and T. Frederico, Phys. Rev. C **92**, 045203 (2015).
[39] R. N. Mishra, H. S. Sahoo, P. K. Panda, N. Barik, and T. Frederico, Phys. Rev. C **94**, 035805 (2016).
[40] H. S. Sahoo, G. Mitra, R. N. Mishra, P. K. Panda, and B. A. Li, Phys. Rev. C **98**, 045801 (2018).
[41] H. S. Sahoo, R. N. Mishra, D. K. Mohanty, P. K. Panda, and N. Barik, Phys. Rev. C **99**, 055803 (2019).
[42] A. Li *et al.*, J. High Energy Astrophys. **28**, 19 (2020).
[43] H. S. Sahoo, S. Karan, R. N. Mishra, and P. K. Panda, Phys. Rev. C **104**, 055805 (2021).
[44] P. K. Panda, A. Mishra, J. M. Eisenberg, and W. Greiner, Phys. Rev. C **56**, 3134 (1997).
[45] P. G. Blunden and G. A. Miller, Phys. Rev. C **54**, 359 (1996); H. Shen and H. Toki, *ibid.* **61**, 045205 (2000); P. K. Panda, R. Sahu, and C. Das, *ibid.* **60**, 038801 (1999); P. K. Panda, M. E. Bracco, M. Chiapparini, E. Conte, and G. Krein, *ibid.* **65**, 065206 (2002); P. K. Panda and F. L. Braghin, *ibid.* **66**, 055207 (2002).
[46] P. A. M. Guichon, J. R. Stone, and A. W. Thomas, Prog. Part. Nucl. Phys. **100**, 262 (2018).
[47] J. R. Stone, P. A. M. Guichon, H. H. Matevosyan, and A. W. Thomas, Nucl. Phys. A **792**, 341 (2007).
[48] T. F. Motta, A. M. Kalaitzis, S. Antić, P. A. M. Guichon, J. R. Stone, and A. W. Thomas, Astrophys. J. **878**, 159 (2019).
[49] W. Husain and A. W. Thomas, *Proceedings of the 14th Asia-Pacific Physics Conference*, edited by T.-Y. Tou, J. Yokoyama, R. A. Shukor, K. Tanaka, H. J. Choi, R. Matsumoto, O.-H. Chin, J. H. Chin, and K. Ratnavelu, AIP Conf. Proc. No. 2319 (AIP, Melville, NY, 2021), p. 080001.
[50] B. P. Abbott *et al.*, Phys. Rev. Lett. **119**, 161101 (2017).
[51] B. P. Abbott *et al.*, Phys. Rev. Lett. **121**, 161101 (2018).
[52] B. P. Abbott *et al.*, Astrophys. J. Lett. **892**, L3 (2020).
[53] H. T. Cromartie *et al.*, Nat. Astron. **4**, 72 (2020).
[54] M. C. Miller *et al.*, Astrophys. J. Lett. **918**, L28 (2021).
[55] T. E. Riley *et al.*, Astrophys. J. Lett. **918**, L27 (2021).
[56] N. K. Glendenning, Phys. Rep. **342**, 393 (2001).
[57] J. R. Oppenheimer and G. M. Volkoff, Phys. Rev. **55**, 374 (1939); R. C. Tolman, Proc. Natl. Acad. Sci. USA **20**, 169 (1934).
[58] G. Baym, C. Pethick, and P. Sutherland, Astrophys. J. **170**, 299 (1971).
[59] M. Ju, X. Wu, F. Ji, J. Hu, and H. Shen, Phys. Rev. C **103**, 025809 (2021).
[60] P. Bedaque and A. W. Steiner, Phys. Rev. Lett. **114**, 031103 (2015).
[61] E. Fonseca *et al.*, Astrophys. J. **832**, 167 (2016).
[62] E. Fonseca *et al.*, Astrophys. J. Lett. **915**, L12 (2021).
[63] E. E. Flanagan and T. Hinderer, Phys. Rev. D **77**, 021502(R) (2008).
[64] T. Hinderer, Astrophys. J. **677**, 1216 (2008).
[65] S. Postnikov, M. Prakash, and J. M. Lattimer, Phys. Rev. D **82**, 024016 (2010).
[66] V. Hambaryan *et al.*, Astron. Astrophys. **601**, A108 (2017).
[67] S. Weissenborn, I. Sagert, G. Pagliara, M. Hempel, and J. Schaffner-Bielich, Astrophys. J. Lett. **740**, L14 (2011).
[68] F. Özel, D. Psaltis, S. Ransom, P. Demorest, and M. Alford, Astrophys. J. Lett. **724**, L199 (2010).
[69] L. Bonanno and A. Sedrakian, Astron. Astrophys. **539**, A16 (2012).